Experimental Analysis of Cavitation Erosion on Blade Root of Controllable Pitch Propeller

Afaq Ahmed Abbasi[a], Michele Viviani[a], Daniele Bertetta [b], Marina Delucchi[a], Rico Ricotti[c] and Giorgio Tani [a,1]
[a] *University of Genoa, 16145, Genoa, Italy*
[b] *Fincantieri S.p.A. Naval Vessel Business Unit, 16000 Genoa, Italy*
[c] *Boero Bartolomeo SpA, 16121 Genoa, Italy*

Abstract. The aim of this study is to experimentally investigate the cavitation erosion on the blade root of a model scale controllable pitch propeller. Tests are carried out in a cavitation tunnel, using the soft paint technique to study cavitation erosion, exploiting also two standard cameras and one high speed camera to study the damage patterns and cavitation dynamics, respectively. Standard cameras are placed on the top of test section in order to periodically monitor the occurrence of damages on the layer of paint. The high-speed camera has been used instead to analyse bubble dynamics and identify potentially erosive phenomena. Three different cavitation bubble structures on the blade root have been identified in the present study: streak cavitation, spherical bubble cavitation, and twisting bubble cavitation. The paint tests results have been analysed together with high-speed videos, showing a remarkable agreement between the occurrence of damage and cavitation collapse phenomena. The results demonstrated two regions on the propeller blade root with high risk of erosion: (1) suction side blade root showed significant damage pattern due to single bubble as well as bubble assembly collapse, and (2) pressure side blade root showed slight damage pattern due to spherical bubble collapse.

Keywords. Cavitation erosion, propeller blade root, soft paint test

1. Introduction

Cavitation is a phenomenon that occurs in flowing systems when the fluid pressure falls below the vapour pressure. At such a low-pressure gas bubbles and air pockets are formed in fluid, these bubbles and pockets travel within the flowing system, and collapse when the pressure returns above the vapour pressure. When collapse occur near to a solid boundary, it impinges cyclic loading on the structure, possibly causing material removal from the surface, i.e. erosion [1], [2].

Cavitation erosion may significantly reduce the operational lifespan of the equipment and increase the maintenance cost. Therefore, naval architects put all their efforts in designing propellers and other appendages in such a way that it avoids cavitation erosion in the operation range.

[1] Corresponding Author, Department of Electrical, Electronic, Telecommunications Engineering and Naval Architecture University of Genoa, Italy; E-mail: giorgio.tani@unige.it

The idea of cavitation damage of the surface by bubble collapse was first proposed by Rayleigh in [3], where empty and vapour filled spherical shaped bubbles at constant pressure in inviscid and incompressible flow were studied. Based on micro-level, cavitation consists of an ensemble of small bubbles of different sizes, which may collapse in the form of spherical symmetrical bubbles or asymmetric bubbles [4]. It has been identified in the literature that bubble collapse can create either shock wave or microjet, based on the shape of bubbles [5]. Research studies investigated numerically and experimentally the collapse of spherical shaped bubble, and concluded that spherical collapse may result in generation of a shock wave [6, 7]. The interaction of shock wave with the solid surface results in increased external stress on the surface and eventually erosion. On the other hand, during the collapse of non-spherical bubbles, the pressure gradient around the collapse is not constant, causing the formation of microjet structure [8]. The microjet structure generates water-hammer or jet cutting pressure on the surface, which severely damages the structure [9].

The characteristics of the bubble collapse are highly dependent on the surrounding flow field and on the closeness of bubble with the solid boundary. In addition, different pressure impulses are generated by the bubble collapse on the boundary or near the solid boundary, which includes pressure pulse during the bubble collapse, the impact pressure from liquid jet formed within the bubble and impulsive pressure from bubble interaction with the radial flow and tiny bubbles present inside fluid [10].

In addition to micro-level bubble collapse, the research has focused on macro-level hydrodynamic phenomena involved in erosive collapse. High speed visualisation and paint tests have been used synchronously to study the macro-level hydrodynamic phenomena within the cavitation erosion [11, 12]. In a macro-level study using high speed visualization, it has been reported that cavitation erosion is contributed by five different structures, which include cloud cavity collapse, horse-shoe vortex collapse, twister vortex collapse, micro-bubbles collapse on the closure of the sheet cavity, and micro-cavities collapse within break-up region of the cloud cavity [13]. It has also been concluded in the same study that cloud cavity collapse is responsible for almost eighty percent of total erosion damages on the surface. In addition, it has been identified in another study that cloud cavitation collapse is closely linked with the probability of cavitation erosion [14].

Experimental investigations have been used to understand the underlying mechanism of cavitation erosion with bubble collapse. In an experimental study by Dular *et al.*, [13], cavitation erosion has been studied by testing an hydrofoil in a cavitation tunnel. The results demonstrated significant relationship between cavitation erosion and cavitation visualisation. Cao et al., studied a twisted foil using paint test and high-speed visualisation, and results revealed severe paint removal and erosion damages in the vicinity of closure line of sheet cavity, as the flow detaches and collapses in that region [15]. Aktas, *et al.* experimentally studied the erosion caused by sheet cavitation on a model propeller using different paint techniques [16].

The study of cavitation erosion on marine propellers is further complicated by the variety of phenomena occurring on propeller blades depending on propeller geometry, loading conditions, propeller inflow conditions etc. The focus of the present study is on the cavitation occurring at blade root of a controllable pitch propeller. Paint tests have been used in parallel with high-speed visualisation to study the damage pattern and cavitation dynamics respectively.

2. Experimental Setup

2.1. UNIGE Cavitation Tunnel and Propeller Model

The experiments were carried out in the cavitation tunnel at UNIGE. This facility is a closed water circuit cavitation tunnel with test section dimensions of height x width x length = 0.57 m x 0.57 m x 2 m. The tunnel is equipped with Kempf & Remmers H39 dynamometer, which measures the thrust, torque, and rate of revolution of the propeller. More details about the tunnel can be found in [17].

The test case for present study is the model of a four blade controllable pitch propeller. The main parameters of the propeller are given in Table 1.

Table 1. Main characteristics and parameters of propeller used in present study

Propeller Diameter	0.23
Pitch Ratio at 0.7R	1.3
Number of Blades	4
Expanded Blade Area Ratio	0.7

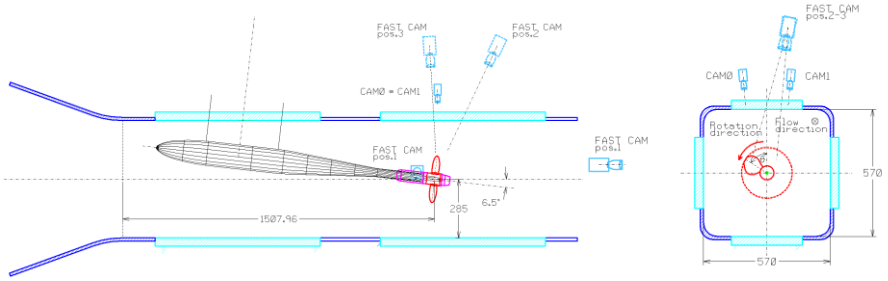

(a) **(b)**

Figure 1. Experimental setup used in present study (a) Longitudinal view (b) Transverse view

The propeller is installed on the dynamometer in pushing configuration, with the shaft inclined by 6.5 degrees and positioned in a way to ensure good optical access from the observation windows of the tunnel. Considered test conditions simulate the typical case of a high speed vessel running at full speed, that is when some blade root cavitation may occur, rising the question about the erosion risk associated with this phenomenon. The total run time of propeller for the test in cavitation tunnel was around 200 minutes.

2.2. Paint Coating

ITTC has recommended a set of guidelines and procedure for painting of propellers for cavitation erosion tests [18]. In the main part of the process, the model is covered by a layer of uniformly applied soft paint and it is subjected to cavitation in the cavitation tunnel for a certain time. Any damage of the paint connected with the action of collapsing cavities should be considered as a risk of erosion occurrences [18].

In the present study the propeller blades have been painted using two different paints, two by two. Different paint types have been tested in the preliminary tests for the selection of best paint types and application technique, which are not reported here for the sake of brevity. In this work, results will be presented only for paint coating which was finally assessed as the best one for these tests, i.e. the *Diagraph GS ink*. The paint was applied on blade 1 and blade 2, coating them with a single layer of paint using spray

gun to ensure uniformity, according to the ITTC procedures. After the application of paint coating, a detailed visual inspection was carried out before starting the tests to ensure the quality of the paint coating. Based on the visual inspection, it can be stated that before the test, the coating was uniform and apparently free of damages that could be confused with erosion damage or that could trigger anomalous cavitation.

2.3. Image Acquisition

Two standard cavitation observation cameras (Allied Vision Tech Marlin F145B2) and one high speed camera (Phantom VEO710L) have been used in the present study. Standard cavitation observation cameras are named as CAM0 and CAM1 in this paper, while Fast Cam will be used for referring the high speed camera.

CAM0 and CAM1 acquired images at resolution of 1392x1040 pixels with s sampling frequency of 10 fps and with the help of stroboscopic lights. These two cameras have been fixed on the top of the test section focusing the back of blade at 90 degrees and face of blade at 270 degrees respectively, as shown in Figure 1. The images acquired with these cameras allows monitoring the paint condition during the experiments.

Fast Cam has maximum resolution of 1280 x 800 pixels and maximum frequency of about 7500 fps at maximum resolution. Three different positions of Fast Cam were used in the present study, in order to characterise suction side and pressure side cavitation, as shown again in Figure 1.

During the experiments, acquisitions were recorded considering these combinations of image size and frame rate: (1) 1280 x 800 pixel, frame rate 7500 fps, (2) 1280 x 400 pixel, frame rate 15000 fps and (3) 1280 x 200 pixel, frame rate 22500 fps and (4) 320 x 200 pixel, frame rate 52000 fps.

3. Cavitation Erosion Results and Discussion

To better understand the cavitation erosion results, it is important to discuss the characteristics of cavitation for present test case. Therefore, in the first sub-section results of cavitation observation and visualization will be presented, and in the next sub-section cavitation erosion results will be discussed.

3.1. Cavitation Observation and Visualisation

The present study is focused on the blade root cavitation. The tested condition is characterised by moderate bubble root cavitation, consisting in one or few separate bubbles occurring at blade root for most of the blade passages (some non cavitating blade passages can be observed as well). The maximum diameter reached by observed bubbles have been approximately estimated to be about 10 mm. Among observed bubbles, three different types of cavitation structures have been identified on blade root: (1) streak cavitation, (2) spherical bubble cavitation and (3) twisting bubble cavitation. High speed visualisation results showed that suction side blade root exhibited these three cavitation bubble typologies, while pressure side blade root exhibited spherical bubble cavitation only. The formation, shape and evolution of bubble structure for all three above mentioned bubbles is exemplified in Figure 2.

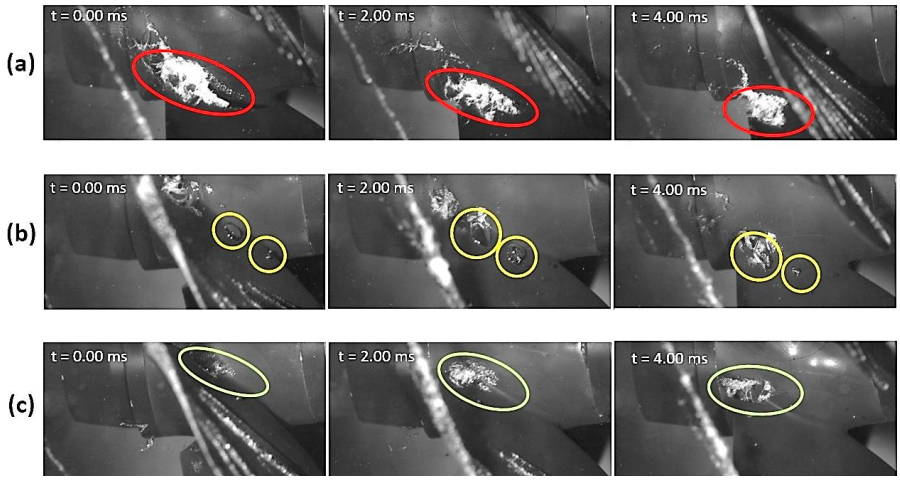

Figure 2. Bubble structures identified on blade root (a) streak cavitation, (b) spherical bubble cavitation and (c) twisting bubble cavitation

Streak cavitation seems to be a result of minor imperfections in the paint surface, not visible by eyes. However, this phenomenon was not present on blades 1 and 2. Spherical bubble cavitation consists of hemi-spherical shaped bubbles, whose shape remains relatively regular during its evolution. The motion of these bubbles seems predominantly a translation motion. Twisting bubble cavitation consists in similar hemispherical bubble whose shape is however stretching along the flow direction. This behaviour seems the results of the combination of translation and rotational motion of the bubbles along their own axis (spinning), as resulting from the bubble being located among layers of fluid with significantly different velocities, as it could reasonably happen close to the blade boundary layer.

3.2. Cavitation Erosion Results

Results of paint tests are here reported with the help of photographs collected by CAM0 and CAM1 during tests. Figure 3 shows the suction side and pressure side of blade root for blade 1 and 2, highlighting paint removal in these zones. The damages observed in the painting of these blades gives a coherent indication of the presence of potentially erosive phenomena. This was later verified analysing the high-speed videos.

- *Suction Side root/Hub* erosion can be seen in the red circles in the images. A consistent damage is observed on blade 1 and blade 2, located between the fillet at the root and the surface of the hub, near the trailing edge of the root itself.

- *Pressure side root* erosion can be seen in the yellow circles. A consistent damage is observed on all the blades, located around the middle of the chord, between the fitting and the surface of the hub.

In order to assess the aggressiveness of the cavitating flow, not only the extent of damages must be analysed, but also its inception time. The periodical inspections of blades during test, both visually and by dedicated cameras, allowed observing the following behaviour:

- *Suction side root cavitation:* a first damage on blade 1 associated with cavitation is observed after about two hours of testing, while a similar damage is observed on blade 2 after about three hours of testing. This difference in terms of damage inception time is

also reflected in the final extent of the damage, as the damage observed on blade 1 is relatively larger than damage of blade 2.

- *Pressure side root:* : Some differences are observed in this case as well, with the appearance of the first damage on blade 1 after almost two and a half hours of testing, followed by a similar damage on blade 2 after three hours of testing.

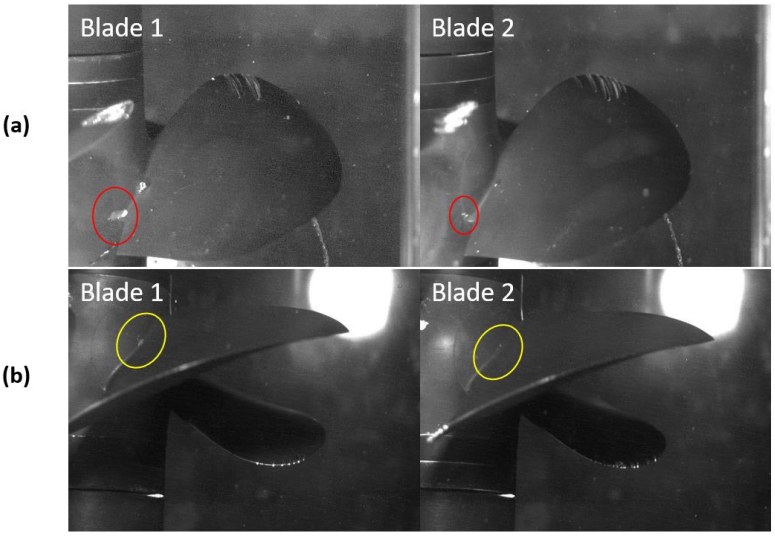

Figure 3. Blade root damages for C1 condition at 199 minutes on (a) suction side and (b) pressure side

In order to better understand the dynamics responsible of observed damages the final stage of the collapse of a cavity is analysed in detail. Figure 4 reports a sequence of frames describing the collapse of a twisting bubble on blade 1. At the beginning of the sequence, a hemispherical cavity, located on the root fillet in correspondence with the trailing edge of the blade can be clearly seen. More precisely, compared to a hemisphere the bubble appears elongated towards the fillet with a small protuberance. The formation of this protuberance is observed in the frames preceding the sequence shown. In fact, it seems to be generated by a sliding effect of the outermost part of the bubble with respect to the portion in contact with the blade surface, a phenomenon that is observed in many cases as a result of the rotational-translational character of the bubble's motion. The latter often results also in the shedding of vortex like structures in the wake, made visible by the cavities generated by the rebound phenomena of the main cavity.

In the next frame (0.33 ms) the beginning of the actual collapse is visible, which occurs with asymmetrical behaviour. Starting from this point, the surface of the bubble contracts in all directions (0.53 ms) until the formation of distinct structures. In the subsequent frames, the collapse of the major cavity is observed, characterized by the acceleration of the bubble surface along a mixed top to bottom and downstream to upstream direction, pointing toward the hub surface. This contraction causes a significant decrease in the volume of the cavity between 0.67 ms and 0.8 ms, until its final collapse at 0.87 ms. The asymmetrical acceleration of the cavity interface toward the hub could be associated with the presence of high velocity microjet. After the main collapse, the formation of new minor cavities due to rebounds and their evolution is observed.

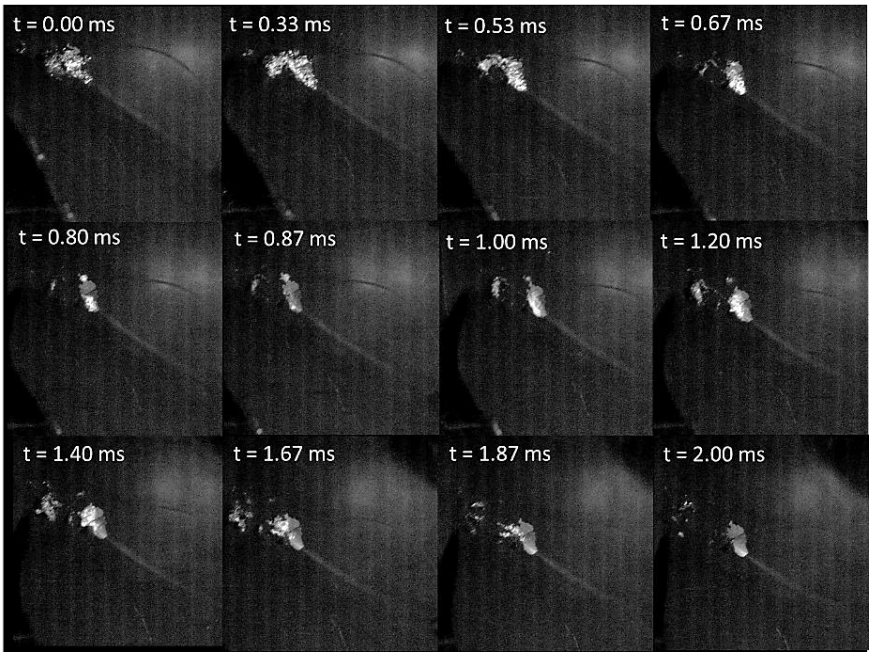

Figure 4. Evolution and collapse of bubble at suction side blade 1 root - fast cam, position 1

The final phase of the collapse just described takes similar form in the case of spherical and twisting bubbles, notwithstanding some differences in the initial phase. Actually, the collapse of large spherical bubbles starts with the formation of a breach in the centre of the bubble, probably associated with a micro jet structure. Then the cavity breaks up into smaller size cavities. Among these cavities, those closest to the hub usually collapse on the hub and root fillet with a behaviour similar to that exemplified in Figure 4 for the twisting bubble. Other minor cavities collapse on the trailing edge of the blade, but with an apparently less violent behaviour. Finally, the remaining cavities collapse downstream. For twisting bubble, significant part of the bubble collapses on the surface of the propeller while for spherical bubble, a lower portion of the initial bubble collapses on the surface. This difference seems indicating larger aggressiveness for twisting bubbles but this conclusion is significantly affected also by the size of the cavities. Beyond this, the videos indicate for most of the cavitation events the presence of cavities collapsing on the hub with a fast contraction of their external surface towards the hub surface, which seems the dominating erosion mechanism for the present case.

Comparing current results with literature, e.g. [13] and [14], the importance of macroscopic bubble collapse is highlighted. Microcavities collapse and cloud cavitation have also been observed during the break-up of the main bubbles and during rebounds. Therefore their contribution to erosion cannot be excluded. The most important consequence of these observations is that driving mechanisms of cavitation erosion can be different depending on the flow problem under study, possibly requiring dedicated treatments.

From the point of view of the global assessment of cavitation erosion for the present case it must be noted that paint removals were observed after significant time. The occurrence of paint removal demonstrates that some of the bubble generated at blade root collapse in correspondence to the propeller surface and that they are characterised by an

energy content sufficient to damage the coating, i.e. they can be considered as potentially erosive. However, the long time needed to observe first damages suggests that erosive bubbles represent a small subset of the total number of bubbles, whose production rate for current condition is rather low (one or few bubbles for blade passage), hence resulting in a relatively low erosive power.

4. Conclusion

In conclusion, the soft paint used in present study showed promising results in detecting considerable damages on both suction and pressure side of blade root, in regions where cavity collapse events occur. Actually, the observed damages were in good agreement with the recorded dynamics of blade root cavitation. Yet, the quantitative assessment of the aggressiveness of cavitation by the presented approach is rather complex. The extent of the damages at the end of the tests, as well as the inception time of the damages can be correlated with intensity of the erosion action, however the accuracy and repeatability of these measures is critical, as confirmed by the differences observed among blades.

High speed videos allowed identifying the erosion mechanism, providing also a valuable support to the results of the paint test. These results stressed the importance of macroscopic cavity collapse among the erosion mechanisms acting for present case, providing valuable indications for following activities on this subject.

The results encourage the continuation of tests on different propellers to study the correlation between damage patterns, inception time and aggressiveness of cavitation.

Form the point of view of the extrapolation of results to full scale, the paint damages observed during model test indicates just a risk of erosion but it does not scale directly to full scale. Following activities will address the problem by different approaches, among which the definition of empirical correlations may represent an attractive solution.

References

[1] Koukouvinis, P., et al., Quantitative predictions of cavitation presence and erosion-prone locations in a high-pressure cavitation test rig. Journal of Fluid Mechanics, 2017. 819: p. 21-57.

[2] Sreedhar, B., S.a. Albert, and A. Pandit, Cavitation damage: Theory and measurements–A review. Wear, 2017. 372: p. 177-196.

[3] Rayleigh, L., VIII. On the pressure developed in a liquid during the collapse of a spherical cavity. The London, Edinburgh, and Dublin Philosophical Magazine and Journal of Science, 1917. 34(200): p. 94-98.

[4] Arabnejad, M.H., et al., Hydrodynamic mechanisms of aggressive collapse events in leading edge cavitation. Journal of Hydrodynamics, 2020. 32(1): p. 6-19.

[5] Franc, J.-P. and J.-M. Michel, Fundamentals of cavitation. Vol. 76. 2006: Springer science & Business media.

[6] Fujikawa, S. and T. Akamatsu, Effects of the non-equilibrium condensation of vapour on the pressure wave produced by the collapse of a bubble in a liquid. Journal of Fluid Mechanics, 1980. 97(3): p. 481-512.

[7] Kim, K.-H., et al., Advanced experimental and numerical techniques for cavitation erosion prediction. Vol. 106. 2014: Springer.

[8] Johnsen, E. and T. Colonius, Numerical simulations of non-spherical bubble collapse. Journal of fluid mechanics, 2009. 629: p. 231-262.

[9] Supponen, O., et al., The inner world of a collapsing bubble. Physics of Fluids, 2015. 27(9): p. 091113.

[10] Tomita, Y. and A. Shima, Mechanisms of impulsive pressure generation and damage pit formation by bubble collapse. Journal of Fluid Mechanics, 1986. 169: p. 535-564.

[11] Bark, G., et al., On some physics to consider in numerical simulation of erosive cavitation. Proceedings of the 7th International Symposium on Cavitation CAV2009. 2009. Ann Arbor, Michiga, USA.
[12] Petkovšek, M. and M. Dular, Simultaneous observation of cavitation structures and cavitation erosion. Wear, 2013. 300(1-2): p. 55-64.
[13] Dular, M. and M. Petkovšek, On the mechanisms of cavitation erosion–Coupling high speed videos to damage patterns. Experimental Thermal and Fluid Science, 2015. 68: p. 359-370.
[14] Van Rijsbergen, M., et al. High-speed video observations and acoustic-impact measurements on a NACA 0015 foil. Proceedings of the 8th International Symposium on Cavitation CAV2012. P2012. Singapore.
[15] Cao, Y., et al. A qualitative study on the relationship between cavitation structure and erosion region around a 3d twisted hydrofoil by painting method. in Fifth International Symposium on Marine Propulsors. 2017. Finland.
[16] Aktas, B., O. Usta, and M. Atlar, Systematic investigation of coating application methods and soft paint types to detect cavitation erosion on marine propellers. Applied Ocean Research, 2020. 94: p. 101868.
[17] Tani, G., et al., Two medium size cavitation tunnel hydro-acoustic benchmark experiment comparisons as part of a round robin test campaign. Ocean Engineering, 2017. 138: p. 179-207 .
[18] ITTC, Recommended Procedures and Guidelines - Cavitation Induced Erosion on Propellers, Rudders and Appendages Model Scale Experiments,. 2011. p. 1-14.